Anal. Bioanal. Electrochem., Vol. 17, No. 1, 2025, 53-66
https://www.doi.org/10.22034/abec.2025.720378

Analytical & Bioanalytical Electrochemistry

Full Paper

Development of New Anodes based on 1,4-Trans Polymyrcene and Carbon Graphite for Microbial Fuel Cells

Youness Tahiri,[1,*] Saliha Loughmari,[2] Mustapha Oukbab,[1] Hassan Haddouchy,[3] Mohamed Oubaouz,[1] Salah Eddine El Qouatli,[3] Marc Visseaux,[4] Abdelaziz El Bouadili,[2] and Abdelilah Chtaini[1]

[1]*Electrochemistry and Molecular Inorganic Materials Team, Faculty of Sciences and Technology, Sultan Moulay Slimane University, Mghilla Campus, BP 523, 23000, Beni Mellal, Morocco*
[2]*Laboratory of Industrial Engineering and Surface Engineering, Applied Chemistry and Environmental Sciences Team, Sultan Moulay Slimane University, FST-BM, P.B. 523,23 000, Beni-Mellal, Morocco*
[3]*Physical Chemistry environment and material, Moulay Ismail University, Faculty of Sciences and Technologies, Boutalamine 52000 Errachidia, Morocco*
[4]*Univ. Lille, CNRS, Centrale Lille, Univ. Artois, UMR 8181, UCCS, Unité de Catalyse et Chimie du Solide, F-59000, Lille, France*

*Corresponding Author, Tel.: +212-678410829
E-Mail: youness.tahiri@usms.ma

Received: 7 November 2024 / Received in revised form: 22 December 2024 / Accepted: 1 January 2025 / Published online: 31 January 2025

Abstract- This study investigates the electrolysis of ethanol in 1 M NaCl using a carbon paste electrode (CPE) modified with trans-1,4-polymyrcene, a polymer known for its catalytic properties. The electropolymerization process was performed using both potentiostatic and galvanostatic techniques, each offering distinct benefits to the electrode's performance. The potentiostatic method produced a uniform polymer layer, enhancing catalytic stability and consistency. Significant improvements were observed with the modified CPE/polymer electrode: double-layer capacitance increased from 4.18 µF/cm² to 603.7 µF/cm², and charge transfer resistance decreased from 40.85 kΩ.cm² to 2.01 kΩ.cm². Galvanostatic polymerization optimized polymer density and morphology, improving surface characteristics. Optical microscopy confirmed the polymer layer's uniformity and ideal thickness, improving ethanol oxidation efficiency due to better electron transfer. The polymer's stability and cost-effectiveness suggest it is suitable for sustainable, repeated use. These results demonstrate the potential of trans-1,4-polymyrcene-modified CPEs for biological catalysis and environmental monitoring, contributing to the development of efficient electrochemical devices.

Keywords- Polymyrcene; Oxidation of ethanol; EIS; Ethanol fuel cell; Staphylococcus

1. INTRODUCTION

The growing demand for alternative energy sources is driven by the threat of geopolitical conflicts and rapid industrial development. These factors are gradually replacing non-renewable energy sources such as fossil fuels and nuclear energy. Conventional energy sources increasingly pose health risks due to their high pollution levels, which negatively affect air and water quality and contribute to global warming. The search for reliable alternative energy solutions is now more critical than ever. Renewable energy sources like solar, hydro, and wind power are central to addressing the energy challenge.

Fuel cells are becoming more attractive for applications that require lower power levels, such as electric vehicles. Two prominent types of fuel cells used in these applications are the hydrogen-air alkaline fuel cell and the methanol-air acid electrolyte fuel cell. However, methanol presents significant health risks due to its toxicity, volatility, flammability, and non-renewable status. Ethanol, on the other hand, stands out as a safer and more promising fuel. It is non-toxic, renewable, and has a higher power density than other alcohols.

A new generation of fuel cells, known as microbial fuel cells, has emerged. These cells use active bacteria as biocatalysts in the anode compartments to generate bioenergy. This study focuses on developing new electrode materials as alternatives to platinum-based electrodes. A carbon paste electrode (CPE) was modified with electrochemically deposited 1,4-trans polymyrcene on its surface. Advances in material science have led to the development of a novel anode combining 1,4-trans polymyrcene and carbon graphite for microbial fuel cells. This innovation uses advanced electropolymerization techniques, including potentiostatic and galvanostatic methods, to improve the electrode's catalytic performance and stability. The electrode also incorporates biological elements, such as Staphylococcus aureus, which forms a biofilm that enhances electrochemical performance. This approach focuses on cost-effectiveness, durability, and the use of renewable materials, supporting sustainable bioelectrochemical technology.

2. EXPERIMENTAL SECTION

2.1. Reagents and apparatus

All chemicals used were of analytical grade and employed without further purification. Solutions were prepared using double-distilled water. Ethanol with 97% purity was sourced from Sigma-Aldrich (USA), while commercial graphite powder was obtained from Carbone, Lorraine, France (ref 9900). Electrochemical measurements were performed using a Voltalab potentiostat (PGSTAT 100 model, Ecochemie B.V., Utrecht, The Netherlands) controlled by Voltalab Master 4 software running on Windows 2007. The electrochemical cell setup included three electrodes: a polymer/CPE working electrode, a platinum counter electrode, and a saturated calomel electrode (SCE) as the reference electrode. Carbon paste electrodes were

prepared by blending high-purity graphite powder with paraffin oil to form CPE, which was then loaded into the electrode cavity. An electrical connection was made using a carbon rod.

The conditions for the three-electrode tests were carefully controlled to ensure precise results. The cell configuration consisted of a polymer/CPE working electrode, a platinum plate counter electrode, and an SCE reference electrode. The electrochemical polymerization of 1,4-trans polymyrcene was carried out in a 1 M NaCl solution using a successive scanning technique. Electrode characterization was done using cyclic voltammetry (CV) and electrochemical impedance spectroscopy (EIS). CV measurements were conducted at a scan rate of 50 mV/s within a potential range of -1.5 V to +1.5 V, while EIS measurements were performed under similar conditions to observe impedance changes.

Scheme 1 illustrates the step-by-step procedure for immobilizing bacteria within a polymer film on an electrode. Initially, the bare electrode represents the unmodified, clean surface, typically composed of conductive materials such as gold, platinum, or carbon, which serves as the foundation for the process. In the second step, a polymer film is deposited onto the electrode, creating a matrix that facilitates bacterial immobilization. The wavy lines depicted in the image symbolize the polymer structure, emphasizing its role in forming a stable interface. Finally, in the polymer-bacteria-electrode stage, bacteria (represented as black dots) are incorporated into the polymer matrix. This immobilization allows the bacteria to interact directly with the electrode surface.

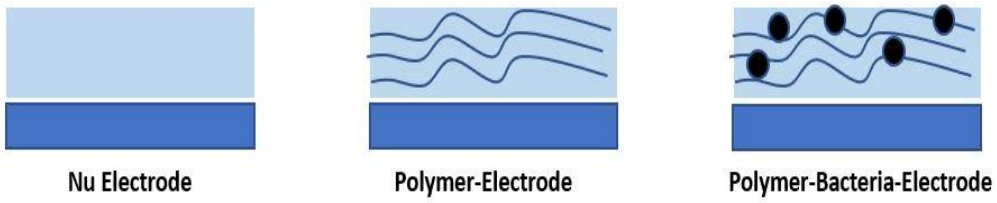

Scheme 1. Procedure for immobilization of bacteria in a polymer film

2.2. Culturing Bacteria

This study used the bacterial strain Staphylococcus aureus, cultivated in Luria-Bertani broth at 37°C for 24 hours. Afterward, the cells were collected by centrifuging at 8400 xg for 15 minutes and washed twice. The cells were then resuspended in a 0.1 M KNO_3 solution. Contact angle measurements were used to evaluate the strain's physicochemical characteristics. To remove oxygen, nitrogen gas was bubbled into the solution for five minutes and then maintained as a protective blanket during the experiment. A fresh solution was prepared for each experiment to ensure reliability. The bacterial suspension was diluted with water to reach the required concentration before use.

2.3. Polymer Synthesis Section

Polymyrcene was prepared using biosourced β-myrcene and neodymium borohydride-based coordination catalysts, paired with n-butylethylmagnesium. The process yielded 1,4-trans polymyrcene (Figure 1) with a production efficiency of up to 84% at 70 °C within 2 hours.

Spectroscopic analysis, including proton nuclear magnetic resonance (^{1}H NMR) (Figure 2a) and carbon-13 nuclear magnetic resonance (^{13}C NMR) (Figure 2b), demonstrated that the synthesized polymyrcene predominantly exhibited a 1,4-trans microstructure, reaching up to 90.8%.

In the ^{1}H NMR spectrum (Figure 2a), signals between 1.50 ppm and 1.75 ppm indicated the presence of CH_3 hydrogens associated with the 1,4-trans unit of polymyrcene. A signal at 2 ppm corresponded to CH_2 protons, while the peak at 5.2 ppm was attributed to olefinic protons linked to the double bonds within polymyrcene.

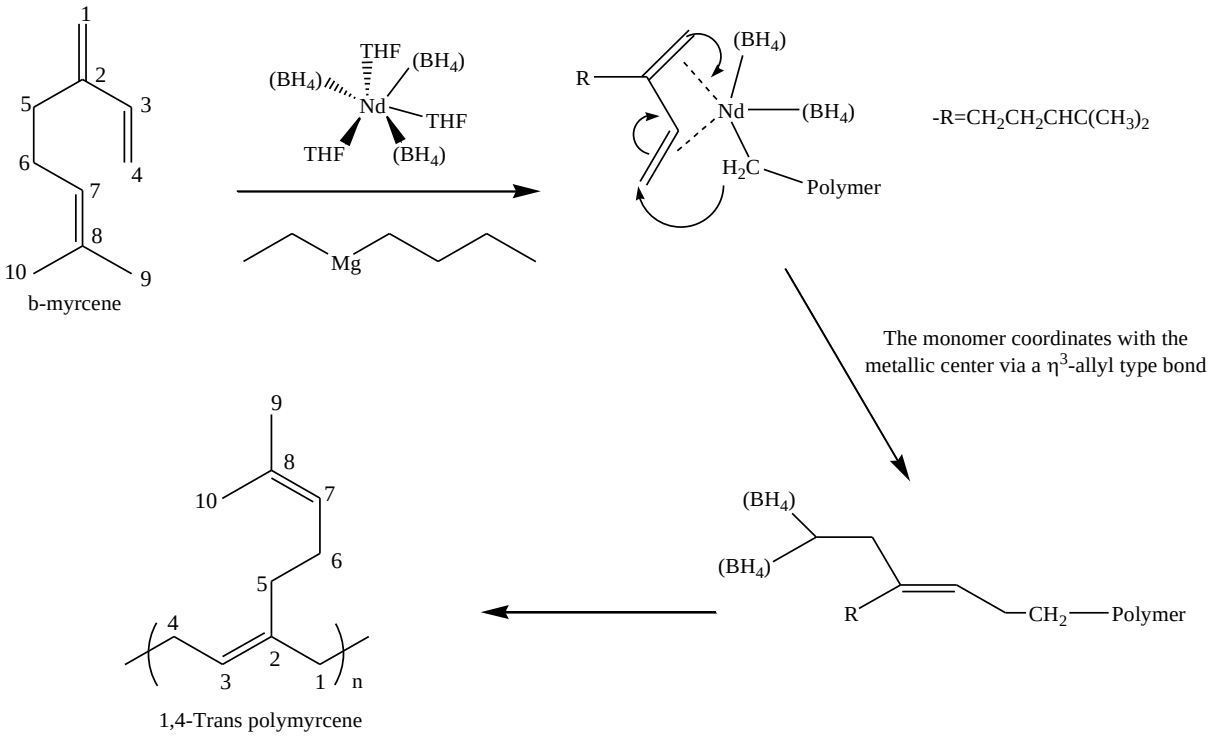

Figure 1. η4 coordination of myrcene, leading to a 1,4 insertion

In the ^{13}C NMR spectrum (Figure 2-b), the structure of 1,4-trans polymyrcene was consistent with ten distinct signals corresponding to the myrcene motif. Six signals were identified as aliphatic carbons (C_1, C_4, C_5, C_6, C_9, and C_{10}), while four signals represented olefinic carbons (C_2, C_3, C_7, and C_8). Among the double bond-associated carbons, quaternary carbons C_2 and C_8 exhibited the highest chemical shifts at 139.36 ppm and 131.80 ppm, respectively. Additionally, CH groups C_3 and C_7 appeared around 124.80 ppm.

In the aliphatic region, CH_3 groups specific to the myrcene motif were identified at C_9 (17.82 ppm) and C_{10} (26.10 ppm). Methylene groups were observed at C_4 (26.99 ppm), C_5 (27.30 ppm), C_6 (30.67 ppm), and C_1 (37.72 ppm).

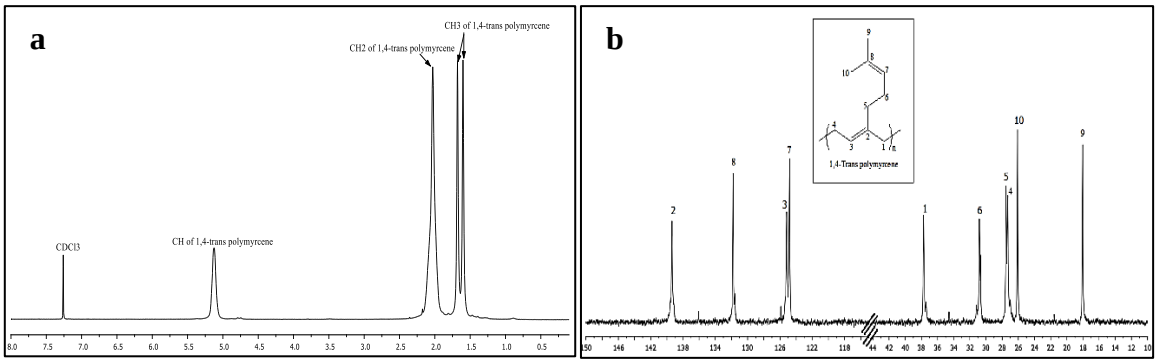

Figure 2. a) ^{1}H NMR, and b) ^{13}C NMR spectrum of polymyrcene

The Steric Exclusion Chromatography (SEC) analysis of the polymer (Figure 3) shows a monomodal distribution, with a polydispersity index (PDI = Mw/Mn; where Mw is the weight average molecular weight and Mn is the number-average molecular weight) of 1.47, indicating a uniform distribution of monomers. This catalytic system produced polymyrcene with a number-average molecular weight (Mn) reaching 3 kg/mol. Differential Scanning Calorimetry (DSC) analysis revealed a glass transition temperature (Tg) of -69.5°C for this polymer.

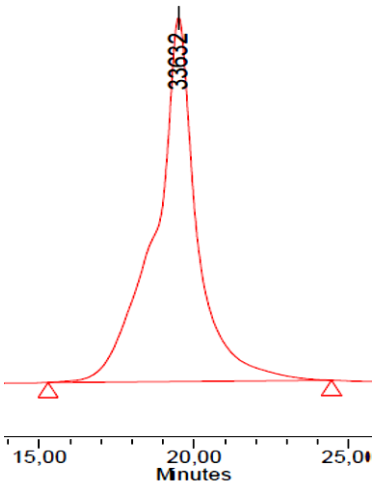

Figure 3. Chromatogram of 1,4-trans polymyrcene

3. RESULTS AND DISCUSSION

3.1. Electrodeposition of polymer

The electrochemical polymerization of 1,4-trans polymyrcene was carried out in a neutral electrolyte solution (1 M NaCl) using a successive scanning technique.

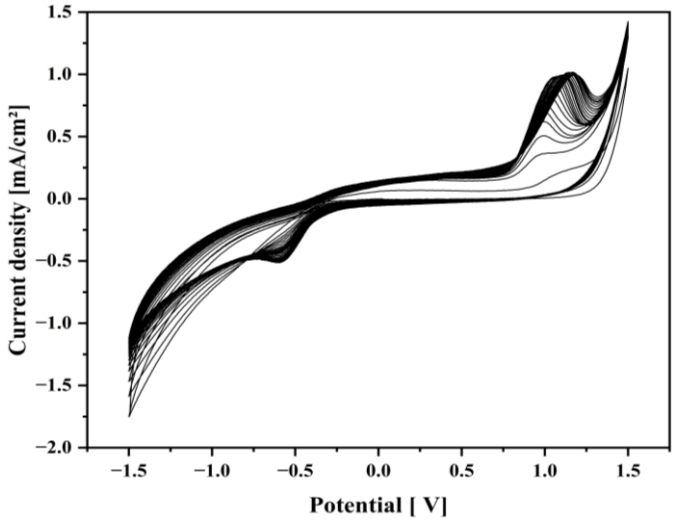

Figure 4. Voltammogram of electropolymerization of 1,4-trans polymyrcene in an electrolyte of 1M of NaCl at pH = 7, on the Al electrode with a scanning speed of 50 mV/s

This approach enabled the creation of stable films, with the deposition rate monitored by tracking the increase in current density. Figure 4 shows a series of voltammograms recorded during the electropolymerization process on a CPE electrode, using a scan rate of 50 mV/s. The experiment took place in a NaCl solution containing 1,4-trans polymyrcene, with the potential range set between -1.5 V and 1.5 V.

The rise in current intensity observed during the cycles indicates the buildup of the polymer film on the CPE electrode surface. As the cycles increase, this suggests that the polymer exhibits conductive properties.

3.2. Surface characteristics

Figure 5 shows an optical microscope image of the CPE/Polymer surface with bacteria. The changes observed on the surface result from bacterial adhesion, leading to the formation of a continuous biofilm.

Figure 5. Images taken by optical microscopy of the elaborated electrodes

3.3. The electrochemical characterization of the CPE and CPE/Polymer

In Figure 6, we analyzed the electrode behavior. A comparison between the cyclic voltammograms of the bare electrode (CPE) and the polymer-modified electrode (CPE/Polymer) shows distinct differences, indicating the modification of the bare electrode. This suggests that the organic polymer molecule was successfully attached to the surface of the carbon paste electrode.

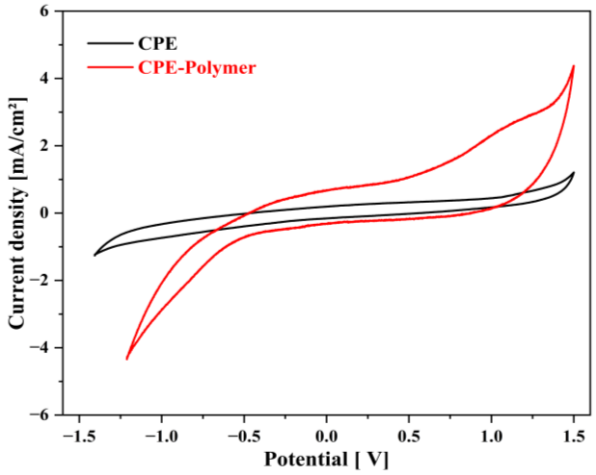

Figure 6. Cyclic voltammograms were recorded on CPE and CPE/Polymer in a 1 M NaCl solution at a scan rate of 50 mV/s

Once the carbon surface is coated with the polymer, there is a noticeable increase in current intensity. This increase is due to the conductive polymer on the working electrode surface. The electroactive species in the polymer facilitate electron transfer, creating conductive pathways between the electrode and the polymer. This combination of polymer and carbon graphite improves electroactive surface areas and accelerates electron transfer.

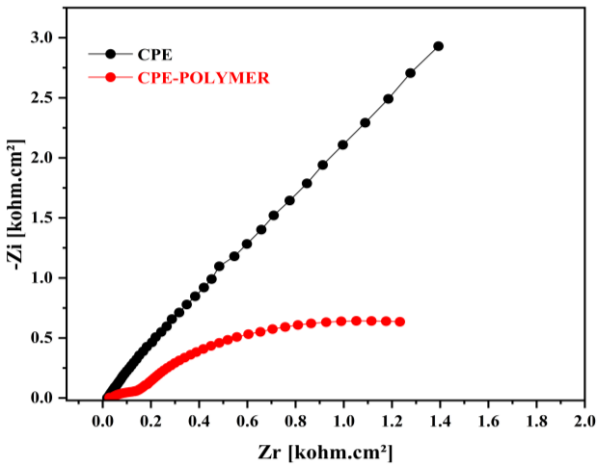

Figure 7. EISs were recorded on CPE and CPE/Polymer in a 1 M NaCl solution at a scan rate of 50 mV/s

Figure 7 shows the electrochemical impedance spectroscopy (EIS) of CPE and CPE/Polymer. Both electrodes display a significant ohmic drop, indicating high electrolyte resistance, which affects the high-frequency region. However, a decrease in total impedance at low frequencies is observed for the CPE/Polymer, likely due to the added capacitance from the polymer film.

Table 1 summarizes the electrochemical parameters obtained from the impedance diagrams. The data shows a significant increase in the double-layer capacitance (C) in the presence of the polymer, indicating that the polymer has been deposited on the surface of the carbon paste electrode (CPE).

Table 1. Electrochemical parameters

Electrode	Diameter kohm.cm²	Coefficient	R_1 kohm.cm²	R_2 kohm.cm²	R_2-R_1 kohm.cm²	C µF/cm²
CPE	40.85	0.999	0.019	38.03	38.01	4.184
CPE/Polymer	2.012	1	0.128	1.876	1.748	603.7

3.4. Immobilization of bacteria on the surface of the CPE/Polymer electrode

Figure 8 shows cyclic voltammograms (CV) from the electrode surface within CPE/Polymer, submerged in a 1M NaCl electrolyte solution, both with and without bacteria. The addition of bacteria causes a noticeable change in the CV profile.

The bacteria studied display redox activity. CV scans taken in the presence of bacteria reveal distinct features, such as a clear cathodic peak at about 1.19 V and a reduction peak during the cathodic scan at around -0.58 V.

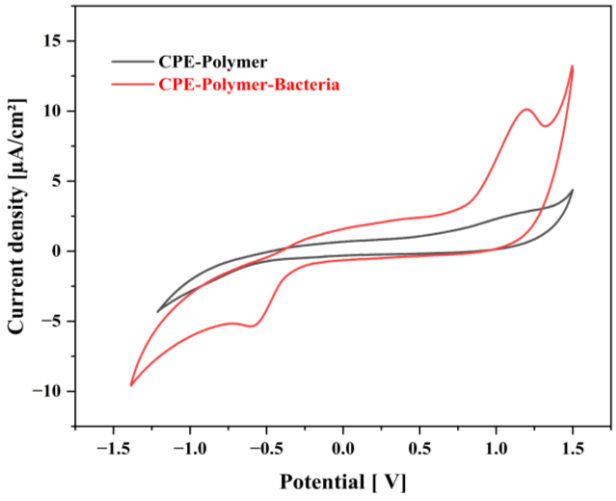

Figure 8. Cyclic voltammograms recorded at CPE/Polymer electrode in the absence and presence of bacteria

Figure 9 shows how bacteria interact with the electrode surface. As contact time increases, the current densities of both the oxidation and reduction peaks increase and shift towards positive and negative potentials, respectively.

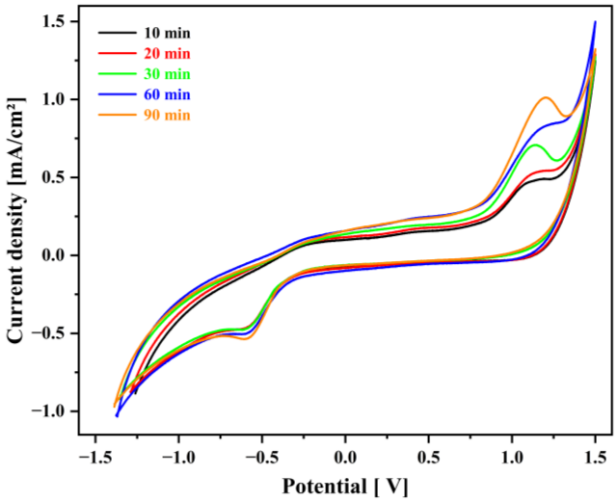

Figure 9. Cyclic voltammograms recorded at CPE/Polymer electrode, in 1 M NaCl solution containing bacteria. Effect of pre-concentration time

An impedance spectroscopy analysis was performed to confirm the findings from the cyclic voltammetry tests. Figure 10 shows the impedance diagram for the CPE/Polymer electrode with bacteria present, immersed in the supporting electrolyte. Electrochemical Impedance Spectroscopy (EIS) highlights diffusion processes at the polymer surface.

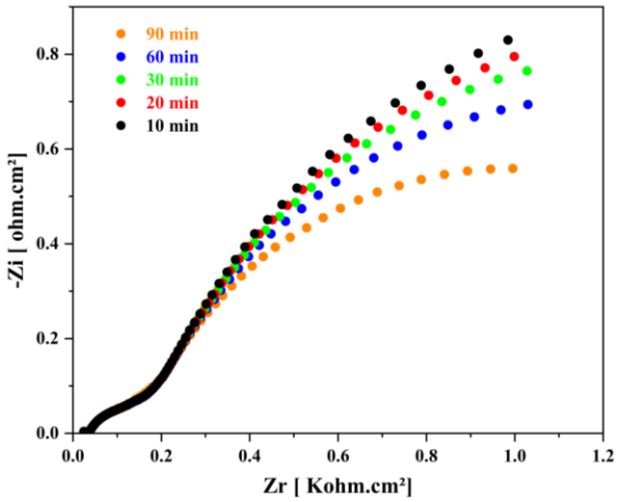

Figure 10. EIS recorded at CPE/Polymer in 1 M NaCl solution containing bacteria. Effect of pre-concentration time

The impedance curves indicate a decrease in charge transfer resistance, suggesting enhanced conductivity of the electrode, likely due to the bacteria on its surface. The

semicircular section diameter represents the electron transfer resistance, which decreases in the presence of bacteria (Table 2). Additionally, a reduction in double-layer capacitance suggests film formation at the Polymer/solution interface.

Table 2. Electrochemical parameters

Contact Time (min)	Diameter kohm.cm²	Coefficient	R_1 kohm.cm²	R_2 kohm.cm²	R_2-R_1 kohm.cm²	C µF/cm²
10	3.318	0.999	0.139	3.021	2.882	526.7
20	3.043	0.999	0.140	2.772	2.632	574.1
30	2.767	0.999	0.145	2.527	2.382	629.6
60	2.408	0.999	0.139	2.200	2.061	723.3
90	1923	0.999	0.131	1.747	1.616	910.6

3.5. Electrooxidation of ethanol on the surface of the CPE/Polymer electrode in the presence of bacteria

The performance of the Polymer/CPE electrode for ethanol oxidation was assessed using cyclic voltammetry. Figure 11 shows the first five cyclic voltammograms, recorded with bacteria and 0.4 mmol of ethanol in the electrolyte solution. A steady increase in current densities is observed with successive cycles, indicating that ethanol oxidation at the Polymer/CPE electrode surface likely occurs through diffusion. The appearance of reduction peaks after the fourth cycle may result from interactions between ethanol and bacteria, leading to the release of the electrode surface.

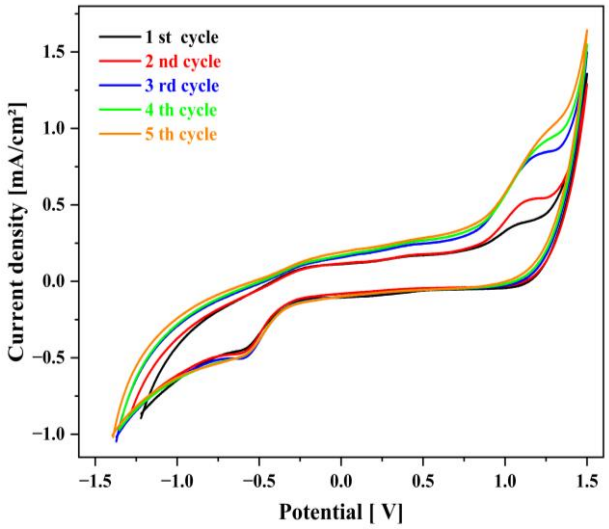

Figure 11. Cyclic voltammograms acquired on Polymer/CPE, in NaCl 1 M solution containing bacteria and ethanol at 50 mV/s, the effect of repeated cycles

This is supported by ethanol's strong bactericidal effect, similar to chlorhexidine, which is highly effective against both Gram-positive and Gram-negative bacteria.

Figure 12 shows significant electrode activity during ethanol oxidation in the presence of bacteria, especially within the first 22 minutes. After this period, the electrode's performance decreases, likely due to film formation blocking active sites. Following 22 minutes, bacterial neutralization of ethanol causes a further reduction in electrode activity.

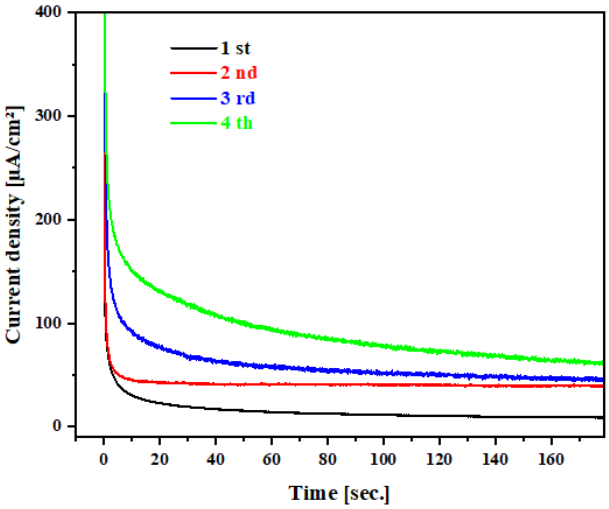

Figure 12. transient curves recorded at Polymer/CPE, in NaCl 1 M solution, containing ethanol and bacteria

An increase in ethanol concentration enhances the current densities for ethanol oxidation on the Polymer/CPE electrode. Higher fuel concentration is linked to an increased catalyst load. Impedance measurements (Figure 13) taken under alkaline conditions support this finding.

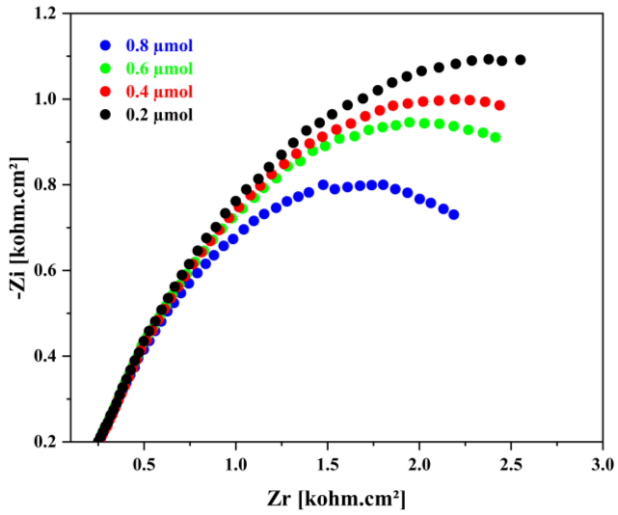

Figure 13. Impedance diagrams recorded for the Polymer/CPE electrode, effect of the variation of the ethanol concentration.

The recorded semicircles decrease as ethanol concentration increases, indicating the electron exchange during the fuel oxidation reaction.

Table 3. Electrochemical parameters

Ethanol µmol/l	Diameter kohm.cm²	Coefficient	R_1 Kohm.cm²	R_2 kohm.cm²	R_2-R_1 kohm.cm²	C µF/cm²
0.2	6.968	1	0.060	4.609	4.549	212.5
0.4	6.103	0.999	0.035	4.630	4.595	220.8
0.6	5.764	0.999	0.036	4.370	4.334	259.2
0.8	5.256	0.999	0.037	4.036	3.999	274.9
1	4.335	0.999	0.038	3.355	3.317	276.2

Figure 14 shows the power density curve for the Polymer/CPE electrode. After reaching 1 µmol/L, the power density levels off, possibly because of catalyst surface saturation.

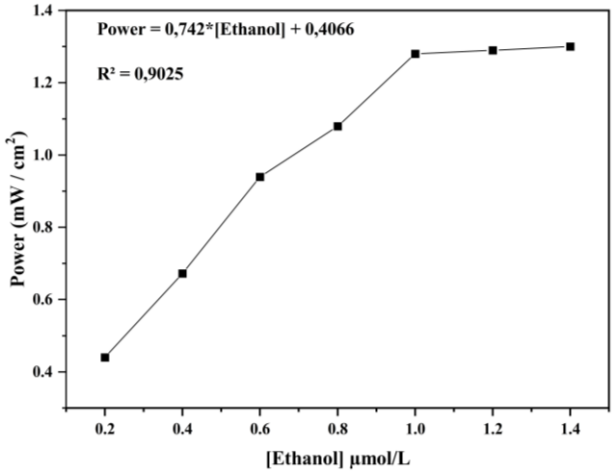

Figure 14. Influence of methanol concentration on power density

4. CONCLUSION

This study designed and tested a novel anode composed of 1,4-trans polymyrcene and carbon graphite for use in microbial fuel cells (MFCs). The innovation lies in using 1,4-trans polymyrcene, a biosourced polymer, to improve the anode's electrochemical properties, facilitating effective ethanol oxidation and bacterial interaction.

Cyclic voltammetry (CV) and electrochemical impedance spectroscopy (EIS) were employed to assess the system’s electron transfer capabilities, surface features, and catalytic

performance. Key parameters examined included double-layer capacitance, charge transfer resistance, and current density during ethanol oxidation.

The results showed significant improvements after incorporating 1,4-trans polymyrcene into the electrode. This modification greatly enhanced the electrode's surface conductivity, yielding a 144-fold increase in double-layer capacitance compared to the unmodified CPE. Electrochemical testing revealed better ethanol oxidation efficiency with higher ethanol concentrations, supported by impedance data indicating lower charge transfer resistance and improved catalytic activity. Additionally, the modified electrode demonstrated increased redox activity in the presence of bacteria, highlighting its potential for bioelectrochemical applications. The electrode also maintained stable performance at ethanol concentrations up to 1 μmol/L, indicating its promising use in microbial fuel cells.

The study focused on ethanol as the fuel and Staphylococcus aureus as the bacterial strain. Future work should explore the anode's performance with other renewable fuels and microbial species. Further research should also assess the long-term stability and real-world performance of the anode. Lastly, integrating this anode into full-scale MFC systems is necessary to determine its practical potential for energy recovery and environmental impact.

Abbreviations

CPE: carbon paste electrode
CV: Cyclic Voltammetry
EIS: Electrochemical Impedance Spectroscopy
DEFC: Direct-ethanol fuel cells
NaCl: sodium chloride
SCE: saturated calomel electrode

Acknowledgments

We thank the Molecular Electrochemistry and Inorganic Materials team at the Beni Mellal Faculty of Science and Technics, Morocco.

Declarations of interest

The authors declare no conflict of interest in this reported work.

Authors' contributions

Youness Tahiri: is the corresponding author; did the experimental protocol; reviewed and edited the original draft of the manuscript; did the modifications asked by the referees and the editor.

Saliha Loughmari, Mustapha Oukbab, Hassan haddouchy, Mohamed Oubaouz, Salah Eddine El Qouatli, Marc Visseaux, and Abdelaziz El Bouadili: contributed to the project supervision, experimental investigation and conceptualization.

Abdelilah Chtaini: acted as supervising professor; elaborated the experimental protocol; wrote the initial draft of the manuscript.

REFERENCES

[1] T. Kåberger, Global Energy Interconnection 1 (2018) 48.
[2] A.A. Yaqoob, K. Umar, R. Adnan, M.N.M. Ibrahim, and M. Rashid, Appl. Nanosci. 11 (2021) 1291.
[3] I. Hanif, B. Aziz, and I.S. Chaudhry, Renew. Energy 2143 (2019) 586.
[4] A.A. Yaqoob, T. Parveen, K. Umar, and M.N. Mohamad Ibrahim, Water 12 (2020) 495.
[5] A. Shahsavari, and M. Akbari, Renewable Sustainable Energy Rev. 90 (2018) 275.
[6] A.Y. Asim, N. Mohamad, U. Khalid, P. Tabassum, A. Akil, D. Lokhat, and H. Siti, Desalination Water Treatment 214 (2021) 379.
[7] N. Kannan, and D. Vakeesan, Renewable Sustainable Energy Rev. 62 (2016) 1092.
[8] O. Enea, A. Chtaini, and D. Duprez, J. Electrochem. Soc. (1993) 1767.
[9] A. Chtaini, D. Duprez, and O. Enea, J. Electrochem. Soc. 138 (1991) 8.
[10] S. Dehbi, H. Massai, and A. Chtaini, Portugaliae Electrochim. Acta 28 (2010) 241.
[11] R.A. Bullen, T.C. Arnot, and J.B. Lakeman, Biosens. Bioelectron. 21 (2006) 2015.
[12] N.M. Sammes, and R. Boersma, J. Power Sources 86 (2000) 98.
[13] L. Carrette, K. A. Friedrich, and U. Stimming, Chem. Phys. Chem. 1 (2000) 162.
[14] B. Seger, and P.V. Kamat, J. Phys. Chem. C 113 (2009) 7990.
[15] B.E. Logan, B. Hamelers R. Rozendal, U. Schröder, J. Keller, S. Freguia, P. Aelterman, W. Verstraete, and K. Rabaey, Environ. Sci. Technol. 40 (2006) 5181.
[16] F.S. Fadzli, M. Rashid, A.A. Yaqoob, M.N.M. Ibrahim, Biochem. Eng. J. 172 (2021) 108067.
[17] S. Dehbi, H. Massai, A. Chtaini, Portugaliae Electrochim. Acta 28 (2010) 241.